Indonesian Physical Review
Volume 07 Issue 03, September 2024
P-ISSN: 2615-1278, E-ISSN: 2614-7904

# Characterization and Electrochemical Behaviour of Boron Doped Diamond in Detecting Amodiaquine

**Hizkia Alpha Dewanto[1], Jatmoko Awali[1], Fadli Hizam[1], Keysi Devain Destiny[1], Irsyad Al Habib[1], Najwa Nabila[1], Murni Handayani[2], Yunita Triana[1]**
[1]*Institut Teknologi Kalimantan, Kalimantan Timur, Indonesia*
[2]*Badan Riset dan Inovasi Nasional, Gedung B.J. Habibie, Jakarta Pusat, Indonesia*

*Corresponding Authors E-mail: nita@lecturer.itk.ac.id*

**Article Info**

***Article info:***
*Received: 21-06-2024*
*Revised: 12-09-2024*
*Accepted: 17-09-2024*

***Keywords:***
*Amodiaquine; Boron Doped Diamond; Limit of Detection; Sensor*

***How To Cite:***
*H. A. Dewanto, J. Awali, F. Hizam, K. D. Destiny, I. Al Habib, N. Nabila, M. Handayani, and Y. Triana, "Characterization and Electrochemical Behaviour of Boron Doped Diamond in Detecting Amodiaquine," Indonesian Physical Review, vol. 7, no. 3, p. 522-537, 2024.*

***DOI:***
*https://doi.org/10.29303/ipr.v7i3.345*

**Abstract**

*Amodiaquine (AQ) is an essential medicine in treating malaria. Yet, the threat of drug resistance and toxicity necessitates accurate measurement of AQ in the human body. This research determines the amodiaquine (AQ) detection performance of boron-doped diamond (BDD) working electrodes. The study utilizes different pulse velocity (DPV) methods to analyze the AQ reaction behavior of BDD. The research demonstrates the reaction mechanism: Two electrons are transferred, and irreversible oxidation reactions occur. The sensor limit of detection (LOD) is measured to determine the performance of working electrodes for AQ detection. The LOD is calculated between 0.0645 μM and 0.3 μM, and changes in analytical concentrations relative to maximum current are calculated. The LOD of the BDD electrode is $1.5\times10^{-8}$ M, lower than previous research on AQ sensors, showing the effectivity of the BDD electrode as an AQ sensor.*



## Introduction

Amodiaquine (AQ) is an antimalarial drug of the 4-aminoquinoline group. This drug is classified as a Mannich base with a similar working mechanism as chloroquine[1]. AQ is highly effective against the erythrocyte phase of four *Plasmodium* species: *falciparum, ovale, vivax,* and *malariae*[2]. It is also used as part of combination therapy with other antimalarial drugs, such as artesunate, to overcome drug resistance in *P. falciparum* infections [3]. Yet, AQ use as the drug has been reduced outside Africa and Asia due to its reported hepatotoxicity [4]. AQ and its metabolite, *N*-desethylamodiaquine, influence the activity of Bcl-2 family proteins,

triggering cell death in human liver cells [5]. Thus, the dosage of AQ medication should be controlled. Combined with the increasing frequency of AQ found in drinking water and sewage systems, which increases the possibility of drug resistance [6], a simple and sensitive sensor system for AQ detection in blood and environment is urgently needed [2], [7].

Previous research has been using various methods to detect AQ quantitatively, using spectrophotometry [8], liquid chromatography [9], fluorimetry [10], conductometry [11], electrophoresis [12], and electrochemical methods. Research using electrochemical methods has been carried out using electrodes made from Platinum Group Elements[7] [2], Multiwalled Carbon Nanotubes (MWCNT) modified by methyl orange and glassy carbon [13], and hemin-based materials [14]. These and other previous research showed electrochemical methods' superiority in AQ detection, mainly short response time, low limit of detection (LOD), higher sensitivity with simple instruments, and high integrability into various systems [15], [16], [17]. Therefore, based on previously reported research results, the electrochemical method has been widely known to provide accurate AQ detection.

Boron-doped diamond (BDD) is one of the electrode materials used in electrochemical sensors. Previously, boron-doped diamond was used to detect dissolved hydrogen sulfide [18] and oxygen in mammal blood [19]. This research shows that BDD sensors, supported by diamond structure, are chemically and mechanically stable[20], unlike other electrochemical sensors, which need time-consuming additional preparations and are inherently unstable [21].

Boron-doped diamond (BDD) is conductive and has excellent properties. Namely, it is a superb electrode that facilitates oxidation, has the largest solvent window of all electrodes, and has a low capacitive current [22]. In electrochemical sensors, BDD is often used as a working electrode; these sensors can be used in dilute or solid electrolytes [20]. BDD is unique as a semiconductor doped with boron. This gives it semi-metallic traits that are good for electrodes [23]. This trait, combined with the solvent window and capacitive current, makes BDD a susceptible sensor [24]. Owing to these advantages, BDD has been applied in various fields, mainly as a gas detector [20].

This research will use BDD to carry out AQ drug detection. First, characterization of BDD was carried out using Raman spectroscopy and SEM. Then, the redox behavior of AQ in 0.1 M acetate buffer solution (ABS) will be studied using cyclic voltammetry (CV) and differential pulse voltammetry (DPV) methods. This observation aims to determine the mechanism of the AQ redox reaction. Then, the scan speed varies from 20 $mV.s^{-1}$ to 100 $mV.s^{-1}$, the potential range of -1 V to +1 V (vs. Ag/AgCl), and the pH range of 2, 3, and 6 are applied. These subsequent experiments are carried out to calculate the sensor's detection limit (LOD) while changing the analyte concentration to the peak current.

## Experimental Method

### A. Production and Surface Characterization of Boron boron-doped diamond Working Electrodes

BDD used in this research is obtained from an endeavor between the Kalimantan Institute of Technology (ITK) and Keio University in Tokyo, Japan, manufactured in the Diamond Electrochemistry Laboratory at Keio University. The BDD electrode is characterized using Raman spectroscopy (Renishaw RM1000) and Scanning Electron Microscopy (JEOL 7400F SEM). First, we prepare the BDD to be tested. Then, the Raman spectroscopy instrument was

used to observe the sample and produce a graph. The graph compared wavelength (Raman shift) and intensity. Raman spectroscopy is used to check the presence of doped diamond and boron structures on the BDD working electrode surface. The steps in SEM testing are sample preparation and observation. The magnifications used for BDD observation are 10.000 x. The purpose of SEM observation is to confirm the polycrystalline diamond structure.

**B. Preparation of Working Electrode**

There are two types of BDD preparation methods: oxygen termination (O-BDD) and hydrogen termination (H-BDD). This research used the H-BDD method due to increased surface electrical conductivity compared to the O-BDD method, resulting in higher sensitivity [23]. The first step of H-BDD preparation is cleaning by soaking the BDD in 15 ml of aqua regia, a mix of $HNO_3$ and HCl with a 1:3 molar ratio, for 1800 seconds. Next, the electrode is rinsed and sonicated with a 40 kHz frequency for 15 minutes in purified water. It was dried with $N_2$ gas. Then, the electrode was cleaned by chronoamperometry using Versa STAT 4 Potentiostat/Galvanostat in 0.1 M $H_2SO_4$. The potential was +3 V (5 minutes) and -3 V (10 minutes), both vs. Ag/AgCl, to optimally produce hydrogen-terminated BDD [25]. The same potentiostat device is used for electrochemical measurement.

**C. Electrochemical Measurements**

Stock solution is prepared by dissolving AQ into 0.5% DMSO solvent until the concentration of 0.1 mM and volume of 1000 mL is reached. The solution is mixed with a 0.1M pH 5 ABS solution and an AQ stock solution with a variation of 10 g. $mL^{-1}$, 15 g. $mL^{-1}$, 20 g. $mL^{-1}$, 25 g.$mL^{-1}$, and 30 g.$mL^{-1}$. The three-electrode systems of the self-fabricated electrochemical cell are linked to the potential window of the -1V to +1V (vs Ag/AgCl), the Ag/AgCl (3 M KCl) reference electrode. Meanwhile, the BDD is the working electrode. The solution volume used in each measurement is 25 ml.

The redox behavior of AQ was meticulously analyzed with a carefully controlled 0.064 M AQ concentration variation in an ABS solution with a pH of 6. The AQ was then carefully analyzed between the analysis concentration and resulting peak current using both CV and DPV techniques with potentials between -1 and +1 (compared to Ag/AgCl). The main analysis principle is the Nernst equation, where the detection limit is acquired from the regression of the equation.

The pH variation was systematically controlled at pH 2, 4, and 6, with 100 $mV.s^{-1}$ scanning speed, and the potential range was -1 V to +1 V (vs Ag/AgCl). The pH variation is intended to observe and evaluate sensor performance under various conditions of solution acidity, mainly acidosis, which is common in malaria patients [26]. The scanning speed was systematically changed from 20 $mV.s^{-1}$ to 100 $mV.s^{-1}$ at pH 6, with potentials ranging from -1V to +1V (vs Ag/AgCl). The variation of scan speed is necessary to calculate the electron number on the reaction of AQ on the BDD surface. These systematic observations aim to find possible shifts, whether a reduction or oxidation of the AQ on the BDD surface. Under the variation of pH level, the control is AQ concentration and scan rate, meanwhile, AQ concentration and pH level become control when scan rate is varied.

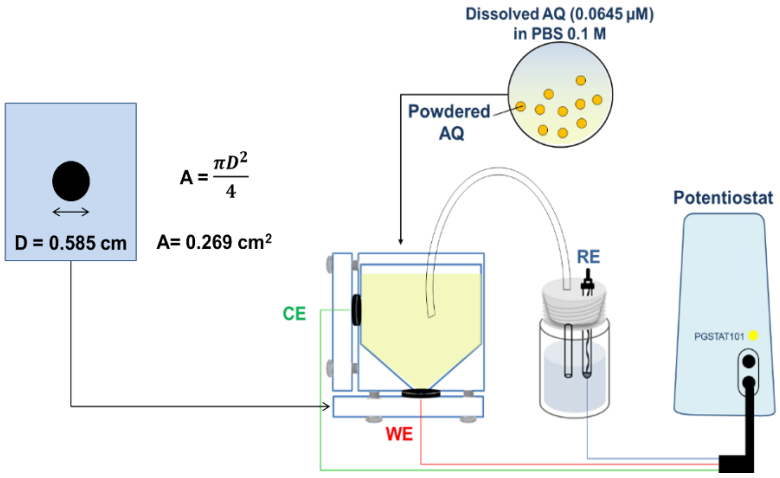


**Figure 1**. The schematics and dimensions of electrochemical analysis set of AQ detection with BDD.

The detection limits vary depending on the AQ concentration of ABS 0.1 M, 10g.mL$^{-1}$ to 30g.mL$^{-1}$. The test uses a scanning speed of 100 mV.s$^{-1,}$ and the range of potential was -1V to +1V (vs. Ag/AgCl) at pH 6. Observation of each concentration was repeated thrice. Thus, the relationship between current density and concentration will be shown as a graph, and then the limit of detection could be calculated using the following equation:

$$LOD = \frac{3.3 \times STD}{Slope} \quad (1)$$

STD is the standard deviation of measured current density, and the slope is the inclination of the linear graph that shows the correlation between current density and concentration.

## Result and Discussion

### A. BDD Surface Structure Analysis

In this study, the surface of the working electrode was characterized to verify the structure and surface composition of the polycrystalline electrode. Raman spectroscopy can identify polycrystalline substances and structures. The result of Raman's observation is shown in Figure 1(A). In addition, it was characterized by scanning electron microscopy. The results of the SEM are shown in Figure 1(B)**.** These characterizations will ensure the purity of the sensor material, which should only contain carbon in the form of diamond and boron as doping elements.

The result of Raman spectroscopy characterizes the chemical composition of the surface of the BDD working electrode. Peaks with notable intensity are at 500 cm$^{-1}$, 1200 cm$^{-1}$, and 1300 cm$^{-1}$, which indicate the presence of carbon sp$^3$, boron, and diamond structure, respectively. No peak was observed at 1600 cm$^{-1}$, which indicates impure carbon sp$^2$. The absence of this peak shows that this BDD is a high-quality BDD. Figure 1(B) shows the polycrystalline structure of the surface of the BDD working electrode. The mean grain size is 5 µm. SEM observation is carried out to observe impurities on the BDD surface. Based on the micrography results, no impurities are observed on the BDD surface.

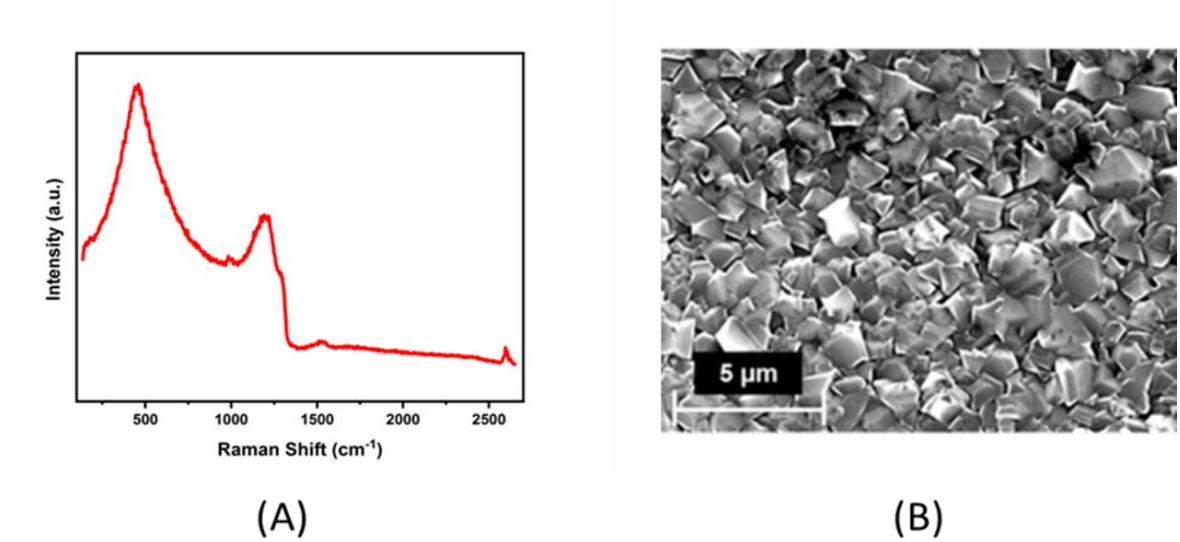


**Figure 1.** The result of Raman spectroscopy (A) and the result from Scanning Electron Microscopy of BDD Working Electrode Surface (B).

### B. Analysis of Amodiaquine Oxidation Behavior on BDD Work Surfaces

Redox behavior analysis is carried out using CV and DPV methods. CV is a widely used electrochemical method that demonstrates the mechanisms of reaction redox, reaction reversibility, and electron transfer kinetics of solvents. DPV is an electrochemical method that measures the difference between currents after potential change [27]. The DPV method has the advantage of having high sensitivity and reduction of the effect of capacitive current [28]. CV methods provide advantages in studying electron transfer in oxidation reactions and are commonly used to analyze chemical species reduction and oxidation processes [29]. Based on the advantages of these two methods, the research uses two voltage meters. CV sampling uses AQ at an ABS concentration of 0.0645 µM, while DPV sampling uses 0.0645 µM.

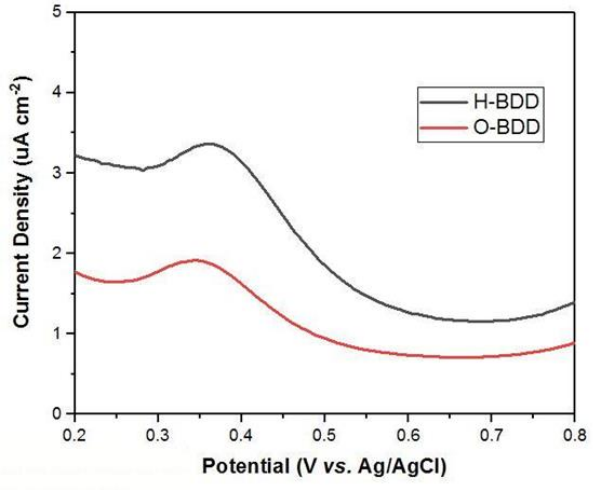


**Figure 2.** Voltammogram of AQ 0.0645 µM in 0.1 M ABS on BDD Work Electrode Surface. The difference between O-BDD and H-BDD is shown.

This research is carried out with a termination process using chronoamperometry techniques and control of the applied potential, namely +3 V for 5 minutes and -3 V for 10 minutes, both

vs Ag/AgCl, in a solution of $H_2SO_4$ 0.1 M. Potential +3 V (vs. Ag/AgCl) is enacted to the termination process with O-BDD oxygen. This termination process aims to obtain a considerable electron affinity value, a stable current, and a vast potential window. Oxygen termination has limitations: it is hydrophilic and has lower conductivity and a negative charge [30]. Terminating hydrogen makes electrode surfaces more conductive. It creates sensitive electrode materials for electrochemical detection [31]. Therefore, a hydrogen termination process is carried out by applying potential -3 V (vs.Ag/AgCl) for a longer time. Apart from that, H-BDD also makes surfaces hydrophobic. This feature makes electrode surfaces more stable. H-BDD can last long in open environments and is effective in liquid ones [32]. The H-BDD and O-BDD processes differ significantly, where the peak current of the H-BDD process is higher. Based on the data above, it is validated that BDD surface termination with H-BDD is more recommended for AQ detection. Then, the redox behavior is analyzed using the CV and DPV methods to produce an AQ of 0.0645 µM in 0.1 M ABS, presented on a voltammogram graph in Figure 3**.**

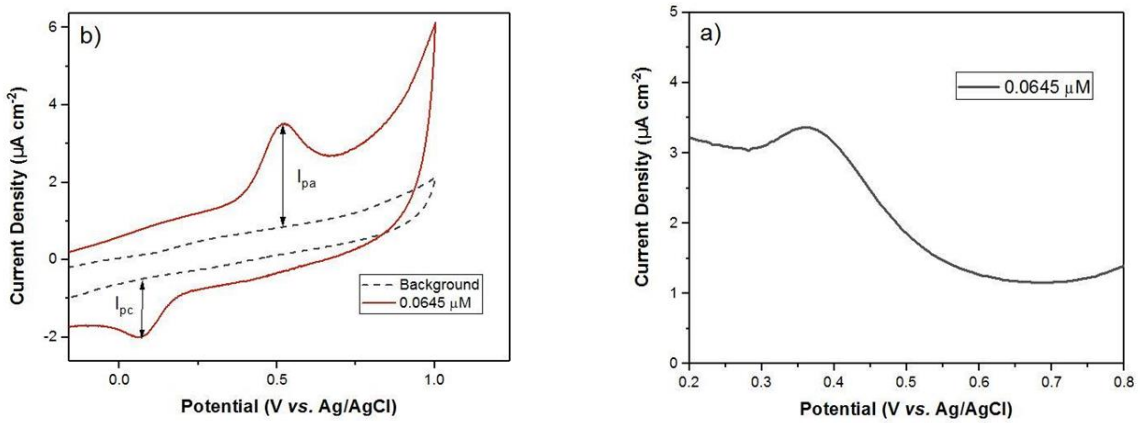


(a) (b)

**Figure 3.** Voltammogram of AQ (a) DPV 0.0645 µM (b) CV 0.0645 µM

Based on the DPV experiment, the range -1 V to +1 V vs. Ag/AgCl background data is obtained using ABS pH 6 samples without AQ content. In Figure 3, no visible current peak indicates no electrochemical reaction in the ABS solvent sample. On the other hand, the 0.0645 µM AQ sample in ABS with the acidity of pH 6 has a peak current at +0.37 V (vs. Ag/AgCl) with a visible oxidation current peak. Besides that, the CV voltammogram also shows the presence of oxidation in the ABS sample. CV experiments in the range -1 V to +1 V obtained a visible peak current at a potential of +0.5 V for the oxidation peak; both are vs Ag/AgCl. Thus, it can be confirmed that the electrochemical method using the BDD working electrode can detect AQ.

### C. Amodiaquine Oxidation Reaction Mechanism on the BDD Working Surface

The variation of the CV technique of scan speed shows the potential change rate per unit time ($mV.s^{-1}$) in one scan cycle [29]. Changes in the scan rate affect the rate of electron flow. The flow happens at the potential that matches the reduction or oxidation potential of the analyte. Then, the electrons in the oxidation process are counted by observing the reaction mechanism using the CV method. Scanning speeds are 20 to 100 $mVs^{-1}$ (with 20 $mVs^{-1}$ interval) in 0.1 M

ABS at pH 6 with a potential range from -1 V to +1 V (vs. Ag/AgCl) at an AQ concentration of 0.0645 µM.

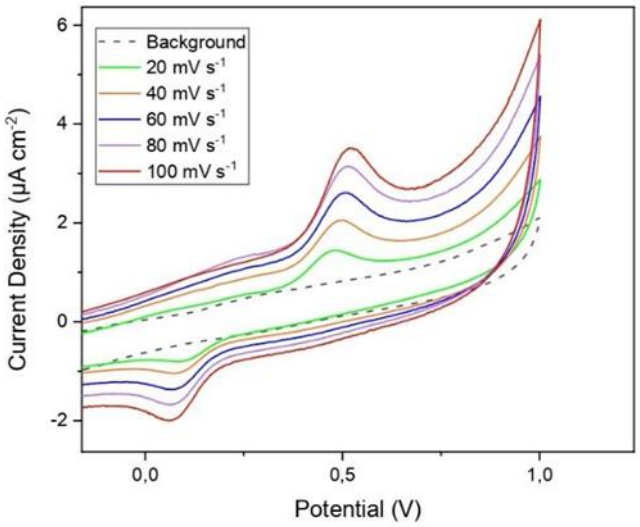


**Figure 4.** The Voltammogram of AQ with Scan Speed Variation

Electrons move from one atom to another. It can also be released (oxidation) and captured (reduction) [33]. Based on measurements using various scan rates, peak oxidation current positively correlates to the scan rate. Figure 4 shows that changes in scan speed affect the peak oxidation current and cause a potential shift, which is caused by the increased scan speed value, and the decrease in the size of the diffusion layer results in a higher current [1]. The concentration of electroactive substances on the electrode surface changes faster and causes an increase in the scan rate. As a result, the peak potential can shift to a more positive or negative value, depending on the electrochemical reaction and the experimental conditions [29][34].

On the other hand, the lower the scan speed, the thicker or farther the start of diffusion layer development from the surface of the electrode, resulting in hampered electron movement characterized by low peak current. The Randles-Sevcik equation can also describe this phenomenon mathematically [35]. In Figure 4, the reversibility properties of a redox reaction are analyzed. Analyzing the peak current value compared to the square root of the scan rate speed can determine an electrochemical reaction's reversibility. Linearity testing between peak current values (Ip) and the square root of the scan speed will determine the reversibility of an electrochemical reaction—Plot Ip vs. $v^{1/2}$, known as the Randles-Sevcik plot.

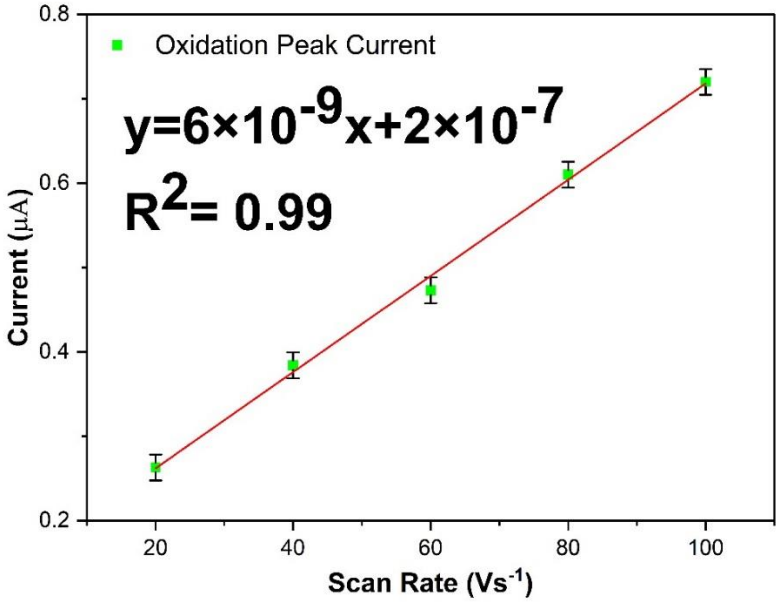


**Figure 5.** Randles-Sevcik oxidation plot of BDD electrode.

Based on Figure 5, the Randles-Sevcik equation obtains the data needed to calculate the electrons transferred. It is used for irreversible reactions [20]. This equation calculates the number of electrons (n) participating in the oxidation reaction on the electrode. This number could be obtained using a calculation that involves maximum measured current (Ip), electrode surface area (A), diffusion coefficient (D), scan rate (v), and concentration of the solution (C). The calculation result is shown in Table 1.

$$Ip = (2.69\times10^{5})\, n\, (an_a)^{1/2} AD^{1/2} v^{1/2} C_A \qquad (2)$$

The surface of the BDD is processed by oxygen and hydrogen terminations to improve the electrical characteristics before observing the redox behavior (Ip - $v^{1/2}$). The final process of the work electrode refers to the finishing process of material treatment, in this case, the surface of the BDD. The termination process of the material is widely applied in various electrochemical material applications, as the termination process can change the electrical properties of the electrode material [36]. BDD working electrodes are processed with oxygen and hydrogen to improve the electrical properties of the surface of the BDD before observing the redox behavior. Termination of the working electrode refers to finishing the material treatment, in this case, the surface of the BDD. The surface termination process of materials is widely used in various materials applications related to electronic chemical issues because the termination process changes the electrical properties of electrode materials [18].

**Table 1.** Calculation of the Randles-Sevcik Equation in Oxide Reactions

| Scan Speed or v ($V.s^{-1}$) | Root Scan Speed ($v^{1/2}$) | Average of Peak Current (A) | Number of Electrons (n) | Average n value |
|---|---|---|---|---|
| 0.02 | 0.14 | $2.63x10^{-7}$ | 2.27 | 2.36 (~2) |
| 0.04 | 0.20 | $3.84x10^{-7}$ | 2.31 | |
| 0.06 | 0.24 | $4.73x10^{-7}$ | 2.31 | |
| 0.08 | 0.28 | $6.1x10^{-7}$ | 2.44 | |
| 0.1 | 0.31 | $1.05x10^{-7}$ | 2.49 | |

In analyzing potential changes in the reaction process above, the DPV method on the surface of BDD is used to determine the effect of the pH of the AQ solution on the reaction mechanism and peak current during the test. This study used three conditions: pH 2, 3, and 6. The pH conditions are adjusted using hydrochloric acid (HCl) as an electrolyte. Based on experiments, the DPV method of changing pH produces an oxidation peak, which is moved along with changes in pH. Under acidity of pH 6, the oxidation point is 0.37 V (Ag/AgCl), the peak current is $7.6\times10^{-4}$ mA.cm$^{-2}$, and under acidity of pH 3, the point is 0.38 V (Ag/AgCl) with a peak current of $7.5\times10^{-4}$ mA.cm$^{-2}$, while in pH 2 the oxidation peak is 0.40 mV with a peak current of $7.0\times10^{-4}$ mA.cm$^{-2}$. Moreover, this can be observed if the current value of acid oxidation is lower than that of alkaline conditions.

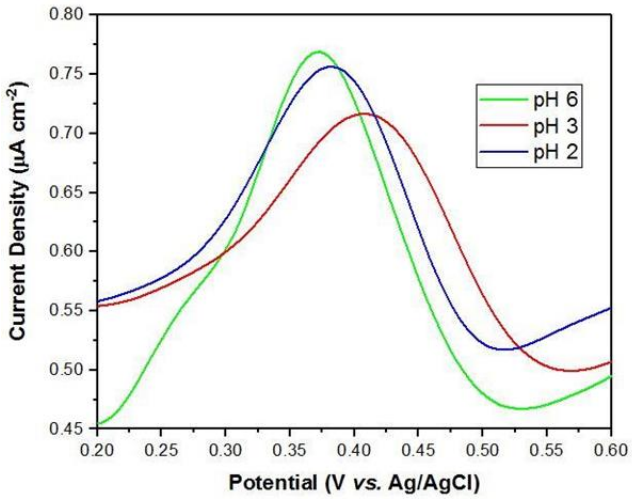


**Figure 6.** Effect of pH on Oxidation Reactions

In potential shift analysis, the phenomenon that occurs when electrochemical reactions are influenced by pH can be explained by the Nernst principle, which describes pH as the concentration of hydrogen [$H^+$]. It is essential to know that hydrogen concentration is logarithmically related to pH value (pH -log [$H^+$]). At low pH, the current decreases as the pH of the solution is reduced in electrochemical measurements, and the peak current becomes smaller. This is due to the increase in the concentration of hydrogen ions ($H^+$) along with the decrease in pH, which can lead to the formation of a diffusion layer around the surface of the electrode. The diffusion layer limits the electrical activity of the electrode surface, restricts the surface's electron transfer path, and reduces the peak current. The pH changes over the peak

current are more pronounced on the reaction side [37]. In addition, the voltammetric measurement of the analyzer also affects the reaction's pH[38].

The drug's chemical composition can trigger potential changes influenced by pH. AQ is a drug with an acid decomposition (pKa) of 8.14–7.8, which is related to the existence of a dimethylamine nitrogen chain and the proton reaction with a quinolone nucleus. This confirms that AQ is a weak diprotic base drug optimal for neutral and alkaline pH solutions [39].

In CV testing, the reaction is reversible, meaning that oxidation and reduction processes occur in the drug compound. Based on analysis of the reaction mechanisms performed, it is estimated that the AQ oxidation reaction is illustrated in Figure 7 [13].

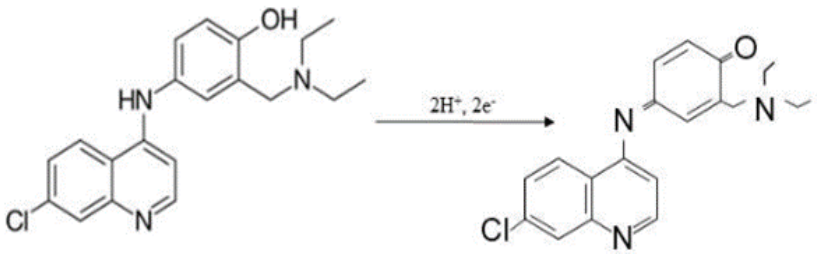


**Figure 7.** Oxidation Reactions in Amodiaquine [13]

**D. Determination of Sensor Detection Limits Limit of Detection (LOD)**

The detection limit (LOD) is determined using the working electrode BDD to detect the AQ content [40]. The determination limit involves changing the AQ concentration value of ABS solution in DPV, with a power of +0V to +1V (Ag/AgCl). Concentrations used were 0.0645 µM, 0.0845 µM, 0.1 µM, 0.2 µM, and 0.3 µM.

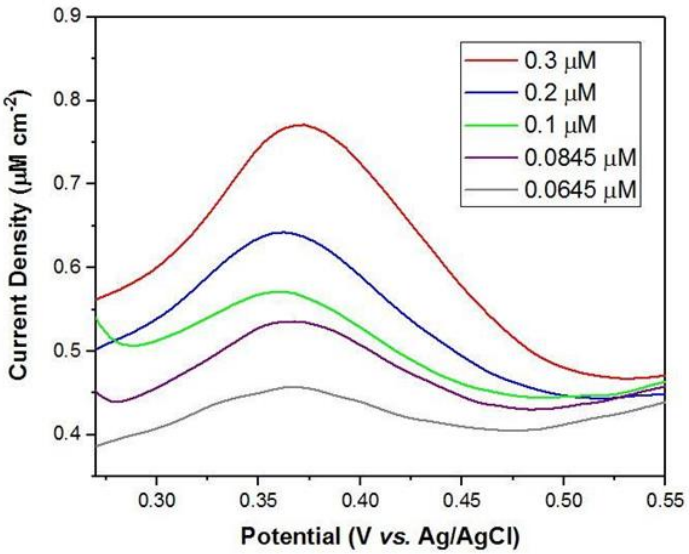


**Figure 8.** Voltammogram of AQ detection using BDD, with varying AQ concentration.

Then, the result of the peak current measurement to the AQ concentration is shown in Figure 9.

The calibration curve plot above shows that the BDD working electrode is a sensor that produces a current response proportional to changes in AQ concentration. The results of a relatively precise linear plot ($R^2$=0.99) showed a gradient value of 1.116. Equation (2) was then used to calculate LOD.

According to the calculations, the detection limit is $1.52\times10^{-2}$ µM ($1.52\times10^{-8}$ M). This value allows the minimum AQ level in the blood to be detected, which is 0.064 M. Other studies have also discovered AQ using different electrodes and electrolytes. Table 2 compares AQ detection limits for various materials. The studies show that BDD is a superior sensor material. This benefit of property arises from the low capacitance of BDD in aqueous solutions [20]. In this case, AQ was detected with higher precision and sensitivity than other electrodes.

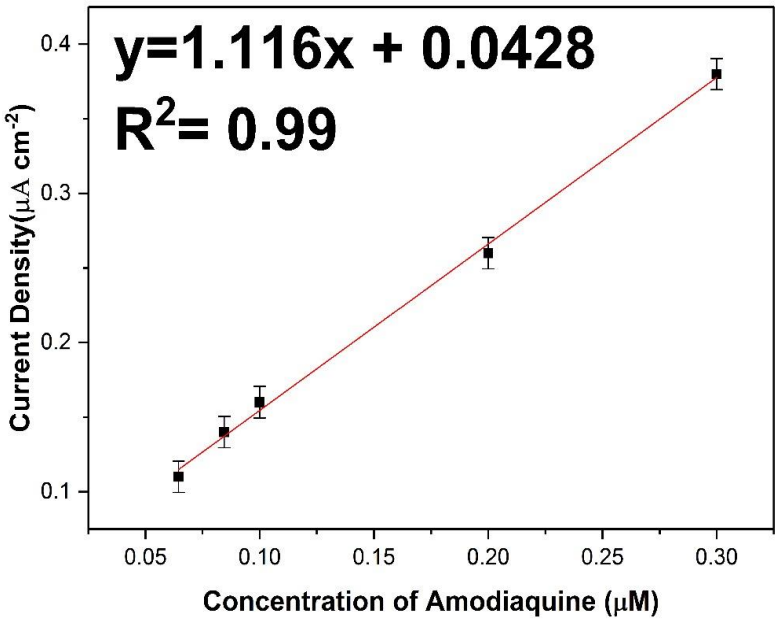


**Figure 9.** The plot of the Current Calibration Curve against the Variation of Concentration

**Table 2.** Research on LOD of AQ using Electrochemical Methods

| Researcher, Year | Working Electrode | Electrolyte | Detection Limit |
|---|---|---|---|
| **This research, 2024** | **Boron doped diamond** | **Acetate buffer solution (ABS)** | **1.52×10-2 µM** |
| [39] | Boron doped diamond | Sodium dodecyl sulfate (SDS) | 6.5×10-2 µM |
| [2] | Pencil graphite electrode | Britton-Robinson Buffer Solution (BRBS) | 0.16 µM |
| [13] | Methyl orange modified glassy carbon electrode & MWCNT | Phosphate Buffer Solution (PBS) | 8.9×10-2 µM |
| [41] | Hemin based electrode | Phosphate Buffer Solution (PBS) | 3.30 µM |
| [42] | PVC membrane | Sodium acetate | 5×10-2 µM |

## Conclusion

This research reported an electrochemical behavior of AQ solution in ABS using a BDD electrode, especially the electrode's performance in measuring various AQ concentrations. It is found that BDD electrodes have superior properties in detecting AQ, mainly in high sensitivity and stability, with lower LOD than previously researched sensors on the same substance. Therefore, it is suggested that BDD electrodes could be implemented to detect the presence of AQ in the human body.

## Acknowledgment

This work is supported by BIMA Kemendikbudristek 2023–2024 research funding by the Ministry of Education, Research and High Education, Indonesia, and Internal Research funding from Institut Teknologi Kalimantan 2024. In addition, the materials get support from Prof. Dr. Yasuaki Einaga, Laboratory of Diamond Electrochemistry, Keio University Japan, and the World Class Professor (WCP) Program by the Ministry of Education, Research and High Education, Indonesia 2022.

## References

[1] C. S. K. Rajapakse *et al.*, "Synthesis of New 4-Aminoquinolines and Evaluation of Their In Vitro Activity against Chloroquine-Sensitive and Chloroquine-Resistant Plasmodium falciparum," *PLoS One*, vol. 10, no. 10, p. e0140878, Oct. 2015, doi: 10.1371/JOURNAL.PONE.0140878.

[2] S. Karakaya, B. Kartal, and Y. Dilgin, "Ultrasensitive voltammetric detection of an antimalarial drug (amodiaquine) at a disposable and low-cost electrode," *Monatsh Chem*, vol. 151, no. 7, pp. 1019–1026, Jul. 2020, doi: 10.1007/S00706-020-02637-Y/METRICS.

[3] R. R. Kinansi and R. Mayasari, "Pengobatan malaria kombinasi artemisinin (ACT) di provinsi Papua Barat tahun 2013," *BALABA: Jurnal Litbang Pengendalian Penyakit Bersumber Binatang*, 2017, doi: 10.22435/blb.v13i1.255.

[4] G. O. Adjei, B. Q. Goka, O. P. Rodrigues, L. C. G. Hoegberg, M. Alifrangis, and J. A. L. Kurtzhals, "Amodiaquine-associated adverse effects after an inadvertent overdose and after a standard therapeutic dose," *ajol.infoGO Adjei, BQ Goka, OP Rodrigues, LCG Høgberg, M Alifrangis, JAL KurtzhalsGhana Medical Journal, 2009•ajol.info*, vol. 43, 2009, Accessed: Aug. 15, 2024. [Online]. Available: https://www.ajol.info/index.php/gmj/article/view/55340

[5] Y. Tang, Q. Wu, F. A. Beland, S. Chen, and J. L. Fang, "Apoptosis contributes to the cytotoxicity induced by amodiaquine and its major metabolite N-desethylamodiaquine in hepatic cells," *Toxicology in Vitro*, vol. 62, p. 104669, Feb. 2020, doi: 10.1016/J.TIV.2019.104669.

[6] T. Rasheed *et al.*, "Environmental threatening concern and efficient removal of pharmaceutically active compounds using metal-organic frameworks as adsorbents," *Environ Res*, vol. 185, p. 109436, Jun. 2020, doi: 10.1016/J.ENVRES.2020.109436.

[7] H. Herlina, M. A. Zulfikar, and B. Buchari, "Cyclic voltammetry in electrochemical oxidation of amoxicillin with Co(III) as mediator in acidic medium using Pt, Pt/Co and Pt/Co(OH)2 electrodes," *MATEC Web of Conferences*, vol. 197, p. 05004, Sep. 2018, doi: 10.1051/MATECCONF/201819705004.

[8] M. T. Ansari, T. M. Ansari, A. Raza, M. Ashraf, and M. Yar, "Spectrophotometric determination of amodiaquinone and sulfadoxine in pharmaceutical preparations," *Chem Analityczna*, vol. Vol. 53, No. 2, pp. 305–313, 2008.

[9] S. K. Sanghi, A. Verma, and K. K. Verma, "Determination of amodiaquine in pharmaceuticals by reaction with periodate and spectrophotometry or by high-performance liquid chromatography," *Analyst*, vol. 115, no. 3, pp. 333–335, 1990, doi: 10.1039/AN9901500333.

[10] F. A. Ibrahim, F. Belal, and A. El-Brashy, "Fluorometric determination of some aminoquinoline antimalarials using eosin," *Microchemical Journal*, vol. 39, no. 1, pp. 65–70, 1989, doi: 10.1016/0026-265X(89)90010-6.

[11] A. S. Amin and Y. M. Issa, "Conductometric and indirect AAS determination of antimalarials," *J Pharm Biomed Anal*, vol. 31, no. 4, pp. 785–794, Mar. 2003, doi: 10.1016/S0731-7085(02)00334-5.

[12] J. P. Mufusama, L. Hoellein, D. Feineis, U. Holzgrabe, and G. Bringmann, "Capillary zone electrophoresis for the determination of amodiaquine and three of its synthetic impurities in pharmaceutical formulations," *Electrophoresis*, vol. 39, no. 20, pp. 2530–2539, Oct. 2018, doi: 10.1002/ELPS.201800170.

[13] T. E. Chiwunze, V. N. Palakollu, A. A. S. Gill, F. Kayamba, N. B. Thapliyal, and R. Karpoormath, "A highly dispersed multi-walled carbon nanotubes and poly(methyl orange) based electrochemical sensor for the determination of an anti-malarial drug: Amodiaquine," *Materials Science and Engineering: C*, vol. 97, pp. 285–292, Apr. 2019, doi: 10.1016/J.MSEC.2018.12.018.

[14] S. Xu *et al.*, "Direct Electrochemistry of Hemin on Graphdiyne Modified Carbon Ionic Liquid Electrode and Electrocatalysis to Bromate," *Int J Electrochem Sci*, vol. 17, no. 11, p. 221122, Nov. 2022, doi: 10.20964/2022.11.39.

[15] Ç. C. Koçak and S. Koçak, "Enhanced Electrochemical Determination of Catechol and Hydroquinone Based on Pd Nanoparticles/Poly(Taurine) Modified Glassy Carbon Electrode," *Electroanalysis*, vol. 32, no. 2, pp. 358–366, Feb. 2020, doi: 10.1002/ELAN.201900500.

[16] B. Aslışen, Ç. C. Koçak, and S. Koçak, "Electrochemical Determination of Sesamol in Foods by Square Wave Voltammetry at a Boron-Doped Diamond Electrode," *Anal Lett*, vol. 53, no. 3, pp. 343–354, Feb. 2020, doi: 10.1080/00032719.2019.1650752.

[17] M. Güneş, S. Karakaya, and Y. Dilgin, "Development of an interference-minimized amperometric-FIA glucose biosensor at a pyrocatechol violet/glucose dehydrogenase-

modified graphite pencil electrode," *Chemical Papers*, vol. 74, no. 6, pp. 1923–1936, Jun. 2020, doi: 10.1007/S11696-019-01036-W.

[18] Y. Triana, M. Tomisaki, and Y. Einaga, "Oxidation reaction of dissolved hydrogen sulfide using boron doped diamond," *Journal of Electroanalytical Chemistry*, vol. 873, p. 114411, Sep. 2020, doi: 10.1016/J.JELECHEM.2020.114411.

[19] Y. Triana, G. Ogata, M. Tomisaki, Irkham, and Y. Einaga, "Blood Oxygen Sensor Using a Boron-Doped Diamond Electrode," *Anal Chem*, vol. 94, no. 9, pp. 3948–3955, Mar. 2022, doi: 10.1021/ACS.ANALCHEM.1C04999/SUPPL_FILE/AC1C04999_SI_001.PDF.

[20] Y. Triana, G. Ogata, and Y. Einaga, "Application of boron doped diamond electrodes to electrochemical gas sensor," *Curr Opin Electrochem*, vol. 36, p. 101113, Dec. 2022, doi: 10.1016/J.COELEC.2022.101113.

[21] Y. Cheng *et al.*, "A review of modification of carbon electrode material in capacitive deionization," *RSC Adv*, vol. 9, no. 42, pp. 24401–24419, Aug. 2019, doi: 10.1039/C9RA04426D.

[22] F. Agustina, A. Y. Bagastyo, and E. Nurhayati, "Electro-oxidation of landfill leachate using boron-doped diamond: role of current density, pH and ions," *Water Science and Technology*, vol. 79, no. 5, pp. 921–928, Mar. 2019, doi: 10.2166/WST.2019.040.

[23] J. V. Macpherson, "A practical guide to using boron doped diamond in electrochemical research," *Physical Chemistry Chemical Physics*, vol. 17, no. 5, pp. 2935–2949, Jan. 2015, doi: 10.1039/C4CP04022H.

[24] Y. Einaga, J. S. Foord, and G. M. Swain, "Diamond electrodes: Diversity and maturity," *MRS Bull*, vol. 39, no. 6, pp. 525–532, 2014, doi: 10.1557/MRS.2014.94.

[25] S. Kasahara *et al.*, "Surface Hydrogenation of Boron-Doped Diamond Electrodes by Cathodic Reduction," *Anal Chem*, vol. 89, no. 21, pp. 11341–11347, Nov. 2017, doi: 10.1021/ACS.ANALCHEM.7B02129/SUPPL_FILE/AC7B02129_SI_001.PDF.

[26] H. Possemiers, L. Vandermosten, and P. E. Van Den Steen, "Etiology of lactic acidosis in malaria," *PLoS Pathog*, vol. 17, no. 1, p. e1009122, Jan. 2021, doi: 10.1371/JOURNAL.PPAT.1009122.

[27] G. V. Guerreiro, A. J. Zaitouna, and R. Y. Lai, "Characterization of an electrochemical mercury sensor using alternating current, cyclic, square wave and differential pulse voltammetry," *Anal Chim Acta*, vol. 810, pp. 79–85, Jan. 2014, doi: 10.1016/J.ACA.2013.12.005.

[28] F. R. Simões and M. G. Xavier, "Nanoscience and its Applications," 2017. doi: 10.1016/B978-0-323-49780-0/00006-5.

[29] N. Elgrishi, K. J. Rountree, B. D. McCarthy, E. S. Rountree, T. T. Eisenhart, and J. L. Dempsey, "A Practical Beginner's Guide to Cyclic Voltammetry," *J Chem Educ*, vol. 95, no.

2, pp. 197–206, Feb. 2018, doi: 10.1021/ACS.JCHEMED.7B00361/SUPPL_FILE/ED7B00361_SI_002.DOCX.

[30] R. Wulandari, "Pengembangan Biosensor Akrilamida Berbasis Hemoglobin Menggunakan Boron Doped Diamond Termodifikasi Nanopartikel," Universitas Bhayangkara Jakarta Raya, Jakarta, 2019. Accessed: Sep. 12, 2024. [Online]. Available: http://repository.ubharajaya.ac.id/24661/1/Retno%20Wulandari-Disertasi-FMIPA-Full%20Text-2019.pdf

[31] C. I. Pakes, J. A. Garrido, and H. Kawarada, "Diamond surface conductivity: Properties, devices, and sensors," *MRS Bull*, vol. 39, no. 6, pp. 542–548, 2014, doi: 10.1557/MRS.2014.95.

[32] J. V. Macpherson, "The Use of Conducting Diamond in Electrochemistry," *Advances in Electrochemical Science and Engineering*, vol. 16, pp. 163–210, May 2016, doi: 10.1002/9783527697489.CH5.

[33] D. Novitasari, "Oksidasi Elektrokimia dengan Menggunakan Anoda Boron Doped Diamond (BDD) pada Lindi Terolah Secara Biologis," Institut Teknologi Sepuluh Nopember, Surabaya, 2019.

[34] R. Martínez-Hincapié, V. Climent, and J. M. Feliu, "Peroxodisulfate reduction as a probe to interfacial charge," *Electrochem commun*, vol. 88, pp. 43–46, Mar. 2018, doi: 10.1016/J.ELECOM.2018.01.012.

[35] Y. Li, F. Xie, C. Yao, G. Zhang, Y. Guan, and Y. Yang, "A DNA tetrahedral nanomaterial-based dual-signal ratiometric electrochemical aptasensor for the detection of ochratoxin A in corn kernel samples," *Analyst*, 2022, Accessed: Jun. 21, 2024. [Online]. Available: https://pubs.rsc.org/en/content/articlehtml/2022/an/d2an00934j

[36] N. Elgrishi, K. J. Rountree, B. D. McCarthy, E. S. Rountree, T. T. Eisenhart, and J. L. Dempsey, "A Practical Beginner's Guide to Cyclic Voltammetry," *J Chem Educ*, vol. 95, no. 2, pp. 197–206, Feb. 2018, doi: 10.1021/acs.jchemed.7b00361.

[37] Fatia Ulfah, "Reversibilitas Reaksi Elektrokimia pada Elektroda Superkapasitor Zeolit Berbasis Silika Sekam Padi yang Dikalsinasi pada Suhu 450, 550, dan 650℃," Bandar Lampung, 2016.

[38] N. Khoiriyah and P. Setiarso, "Modifikasi Elektroda Pasta Karbon dengan Antrakuinon untuk Identifikasi Nikotin pada Rokok Komersial," *Sains dan Matematika*, vol. 5, no. 1, pp. 1–6, 2016, Accessed: Jun. 21, 2024. [Online]. Available: https://journal.unesa.ac.id/index.php/sainsmatematika/article/view/6176

[39] S. K. Kamal and Y. Yardım, "Voltammetric Determination of Anti-Malarial Drug Amodiaquine At a Boron-Doped Diamond Electrode Surface in an Anionic Surfactant Media," *Macedonian Journal of Chemistry and Chemical Engineering*, vol. 41, no. 2, pp. 163–174, 2022, doi: 10.20450/MJCCE.2022.2565.

[40] Y. Zhao *et al.*, "An electrochemical sensor for selective determination of sulfamethoxazole in surface water using a molecularly imprinted polymer modified BDD electrode," *Analytical Methods*, 2015, doi: 10.1039/c4ay03055a.

[41] S. Xu *et al.*, "Direct Electrochemistry of Hemin on Graphdiyne Modified Carbon Ionic Liquid Electrode and Electrocatalysis to Bromate," *Int J Electrochem Sci*, 2022, Accessed: Jun. 21, 2024. [Online]. Available: https://www.sciencedirect.com/science/article/pii/S1452398123026494

[42] M. M. Zareh, K. Elgendy, A. A. Keshk, M. Zaky, and A. Abd-Alhady, "Preparation of Cu-PVC membrane electrochemical membrane sensor based on β-Cyclodextrin," *Int J Electrochem Sci*, vol. 16, no. 12, p. 21123, Dec. 2021, doi: 10.20964/2021.12.41.